Bioorganic & Medicinal Chemistry Letters 19 (2009) 54–57

Contents lists available at ScienceDirect

Bioorganic & Medicinal Chemistry Letters

journal homepage: www.elsevier.com/locate/bmcl

Discovery of novel spirocyclopropyl hydroxamate and carboxylate compounds as TACE inhibitors

Zhuyan Guo [a,*], Peter Orth [a], Shing-Chun Wong [a], Brian J. Lavey [a], Neng-Yang Shih [a], Xiaoda Niu [b], Daniel J. Lundell [b], Vincent Madison [a], Joseph A. Kozlowski [a]

[a] Department of Chemistry, Schering-Plough Research Institute, 2015 Galloping Hill Road, Kenilworth, NJ 07033-0539, USA
[b] Department of Inflammation, Schering-Plough Research Institute, 2015 Galloping Hill Road, Kenilworth, NJ 07033-0539, USA

ARTICLE INFO

Article history:
Received 17 September 2008
Revised 5 November 2008
Accepted 10 November 2008
Available online 14 November 2008

Keywords:
TACE
TACE inhibitors
Hydroxamates
Carboxylates

ABSTRACT

We have discovered nanomolar inhibitors of TNF-α convertase (TACE) comprised of a novel spirocyclic scaffold and either a carboxylate or hydroxamate zinc binding moiety. X-ray crystal structures and computer models of selected compounds binding to TACE explain the observed SAR. We report the first TACE X-ray crystal structure for an inhibitor with a carboxylate zinc ligand.

Tumor necrosis factor-α (TNF-α) is a major immunomodulatory and proinflammatory cytokine that has been implicated in various autoimmune disorders such as rheumatoid arthritis, Crohn's disease, and psoriasis. The success of anti-TNF biologics such as Enbrel® and Remicade® has led to an intensive search for orally active small molecules that suppress TNF-α activity.[1,2] One way of doing so is to block release of TNF-α through the use of small molecule inhibitors of TNF-α converting enzyme (TACE/ADAM17), the metalloprotease that processes the 26 kDa membrane-bound pro-TNF-α to its 17 kDa soluble component.[3]

An early crystallographic structure of a peptidic hydroxamate inhibitor bound to TACE shows that the active site cleft of TACE shares many features with the matrix metalloproteinases.[4] These similarities include an active site zinc coordinated to three histidine side chains, a hydrophobic S1′ pocket adjacent to it and hydrogen bond donors/acceptors such as the carboxylate group of E406 and the backbone amide group of G349. However, one distinguishing feature of TACE is a tunnel interconnecting S1′ and S3′ into a single large cavity. Therefore, TACE selectivity may be achieved by incorporating large substituents on P1′ that can not be accommodated in the smaller S1′ of MMPs. A selective TACE inhibitor is desirable because it may avoid the musculoskeletal side effects that have been reported for broad-spectrum and partially selective MMP inhibitors.[5–7]

Based on crystal structure information on TACE-inhibitor interactions, we have carried out a structure-based design approach to discover novel, potent TACE inhibitors. Key features in the design of TACE inhibitors include a ligand binding to the active site zinc, hydrogen bonding to the catalytic Glu406 carboxylate, a hydrogen bond donor that coordinates to the backbone C=O of Gly349, a hydrogen bond acceptor that coordinates to the backbone NH of Gly349 and/or Leu348, and finally a large hydrophobic P1′/P3′ group for binding to the combined S1′/S3′ pocket. Each of these components is placed on a rigid scaffold that locates each functional group in the appropriate position in the enzyme. In separate papers, we have reported hydroxamate inhibitors based on a cyclopropyl scaffold, which led to the discovery of inhibitors with low nanomolar potency.[8,9] As demonstrated on IK682 and also applied to these compounds, the quinoline group was found to bind to the S3′ subsite thereby conferring excellent selectivity against several MMPs.[10,11] Crystal structures of these inhibitor complexes with TACE reveal an induced fit to the large quinoline S3′ group as a key feature of the potency and selectivity of these inhibitors.

The spirocyclopropyl scaffold disclosed here is a ring constrained analog of the earlier cyclopropyl compounds (Table 1). The synthesis is described in Scheme 1. It was hoped that in addition to projecting the zinc binding group and the hydrogen bonding acceptors/donors into the desired positions, this scaffold would project the P1′ phenyl ring into the S1′ pocket in an orientation similar to that of the potent and selective TACE inhibitor IK682. On the other hand, modeling indicates that cyclization would make the P1′ group move further toward the P3′, which

* Corresponding author. Tel.: +1 908 740 3796.
E-mail address: zhuyan.guo@spcorp.com (Z. Guo).

0960-894X/$ - see front matter © 2008 Elsevier Ltd. All rights reserved.
doi:10.1016/j.bmcl.2008.11.034

Table 1
SAR of hydroxamate-cyclopropyl compounds and IK682

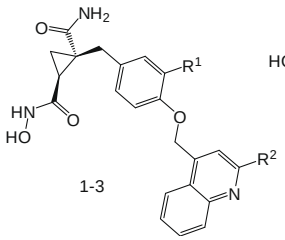

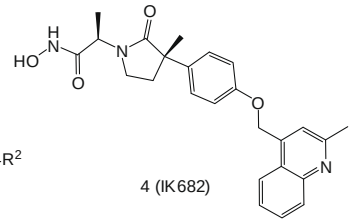

Compound	R^1	R^2	TACE K_i (nM)
1	F	Phenyl	0.14
2	H	Phenyl	0.18
3	H	CH_3	3
4			0.06

The compounds were tested in a FRET assay using the catalytic domain of TACE.

would weaken the pi–pi interactions between the P1′ phenyl and the side chain of His 405, as well as causing steric crowding of the phenyl group with Ala439. Since the quinoline group has been found to render excellent TACE selectivity, it was used throughout the spirocyclopropyl series.

The synthesis of the spirocyclopropyl hydroxamate uses chemistry worked out previously for N-Boc-2-pyrrolidinones and applies it to succinamide in order to prepare compounds **12–18**.[12] Accordingly, compound **5** was converted to the corresponding Gringard reagent then reacted with succinamide. Reduction with sodium cyanoborohydride gave **6**. Alkylation with Eschenmoser's salt followed by elimination gives α,β-unsaturated lactam **8** which can be converted to the corresponding spirocyclopropane **9** using sulfur ylide chemistry. Debenzylation of the phenol, followed by alkylation with a quinoline chloride affords **10**. The ester and amide functionalities are then unmasked with TFA and the resulting compound is converted to the hydroxamate **11** using standard coupling conditions and acid deprotection.

As shown in Table 2, the hydroxamate-spirocyclopropyl compounds **12–18** are potent TACE inhibitors with K_is in the nanomolar range. However, these compounds are less potent than the corresponding hydroxamate-cyclopropyl compounds by 10- to

Table 2
SAR for spirocyclopropyl series

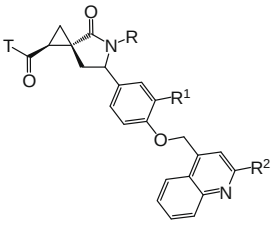

Compound	T	R	R^1	R^2	TACE K_i (nM)
12	NHOH	H	F	Phenyl	6.7
13	NHOH	H	H	Phenyl	30
14	NHOH	H	H	3-Pyridinyl	32
15	NHOH	H	H	CH_3	32
16	NHOH	H	H	4-Pyridinyl	33
17	NHOH	H	H	CF_3	53
18	NHOH	CH_3	F	Phenyl	137
19	OH	H	F	Phenyl	40
20	OH	CH_3	F	Phenyl	94
21	OH	H	H	Phenyl	143
22	OH	H	H	4-Pyridinyl	673
23	OH	H	H	CF_3	2140
24	OH	H	H	CH_3	3070
25	OH	H	H	3-Pyridinyl	3220
26	OCH_3	CH_3	F	Phenyl	>50,000

All the analogs were prepared and tested as racemic mixtures.

100-fold. For example, compound **12** (K_i = 6.7 nM) is 50-fold less potent than compound **1** (K_i = 0.14 nM), and compound **13** (K_i = 30 nM) 100-fold less potent than **2** (K_i = 0.18 nM). While in the cyclopropyl series, 2-phenyl-quinoline increases potency by >10-fold compared with 2-methyl-quinoline (e.g., compounds **3** vs **2**), the potency remains the same in the hydroxamate-spirocyclopropyl series (e.g., compounds **13** vs **15**). Replacing the phenyl with a pyridine does not affect potency, as shown in compounds **14** and **16**. In addition, compound **12** with R^1 as *m*-fluoro-phenyl increases potency by 5-fold, although in the cyclopropyl series the potency remains the same. Due to the limited space in S1′, substitutions on the phenyl ring with a group larger than fluorine are expected to cause steric crowding and to lose potency, as has been observed in the cyclopropyl series.[9] *N*-methyl substitution of com-

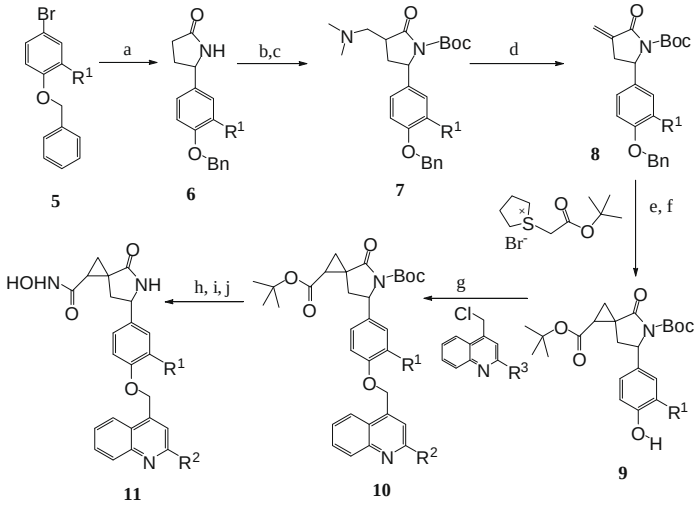

Scheme 1. Reagents and conditions: Yields shown are for R^2 = H, R^2 = phenyl. (a) i—Mg/THF; ii—succinamide; iii—$NaCNBH_3$ (5% over three steps); (b) i—LDA/THF; ii—Boc_2O (68%); (c) i—LiHMDS; ii—Eschenmoser's salt (21%); (d) i—CH_3I/MeOH; ii—$NaHCO_3$ (97%); (e) sulfur ylide/DBU/CH_3CN (40%); (f) $Pd(OH)_2/H_2$ (98%); (g) Cs_2CO_3; aryl chloride (75%); (h) TFA/CH_2Cl_2 (84%); (i) trityl-ONH_2/EDC/HOBT (59%); (j) TFA/Et_3SiH/CH_2Cl_2 (78%). When R = *N*-methyl then *N*-methyl succinamide is used in step a and step b is not performed. When R^1 = F, the same sequence of reactions is used with fluorinated **5**. All final compounds are racemic.

pound **18** decreases potency by 20-fold. Modeling indicates possible steric crowding of the *N*-methyl group with the C=O of Gly346.

Generally speaking, carboxylate is a much weaker zinc ligand than hydroxamate.[13] In the cyclopropyl series, replacing the hydroxamate with carboxylate rendered the compounds inactive (>1000-fold loss in potency, data not shown). A computational study of the binding of zinc ligands showed that the requirement for protonation of Glu406 or the ligand carboxylate is the primary cause of this reduced affinity.[14] However, in the spirocyclopropyl series, the K_is are reduced by only 5- to 100-fold upon substituting carboxylate for hydroxamate. For example, compounds **19** (K_i = 40 nM) and **12** (K_i = 6.7 nM) only differ by 6-fold, and compounds **21** (K_i = 143 nM) and **13** (K_i = 30 nM) by 5-fold. In addition, 2-phenyl-quinoline increases the potency by 20-fold compared with 2-methyl-quinoline (e.g., compounds **21** vs **24**). Compounds **19** and **20** have comparable potency which means that methyl substitution of the lactam is well tolerated. Finally, as expected converting the carboxylate to a methyl ester rendered compound **26** inactive. Compounds **12**, **13**, **17**, **19**, **21**, and **23** showed IC_{50} values in a human whole blood assay for TNF production of greater than 100 micromolar.[15] Due to the lack of activity in the human whole blood assay, compounds were not resolved into their enantiomers or tested for selectivity against other MMPs.

Figure 1 shows the crystallographic structure of compound **21** binding to a TACE mutant enzyme (V353G).[16] The carboxylate group binds to the zinc in a bidentate fashion with O–Zn distance of 1.9 and 2.5 Å, respectively. The weaker zinc-binding oxygen also makes a hydrogen bond with the side chain of Glu406. Here the carboxylic acid of Glu406 is expected to be protonated.[14] The carbonyl oxygen of the lactam makes a hydrogen bond with the backbone NH of Leu348. A crystal water is present as a bridge for hydrogen bonding between the lactam NH and the C=O of Gly346. Modeling indicates that this water molecule would be displaced by the *N*-methyl substitution of compound **20**. The methyl group would then make hydrophobic contacts with the side chains of Ala439 and Leu348. Therefore, the gain in hydrophobic interactions balances the loss of hydrogen bonding. This is consistent with the comparable potency observed in compounds **19** and **20**. In contrast, modeling indicates that the lactam NH in the hydroxamate-spirocyclopropyl series is involved in direct hydrogen bonding interactions with the C=O of Gly346 and that *N*-methyl substitution would cause

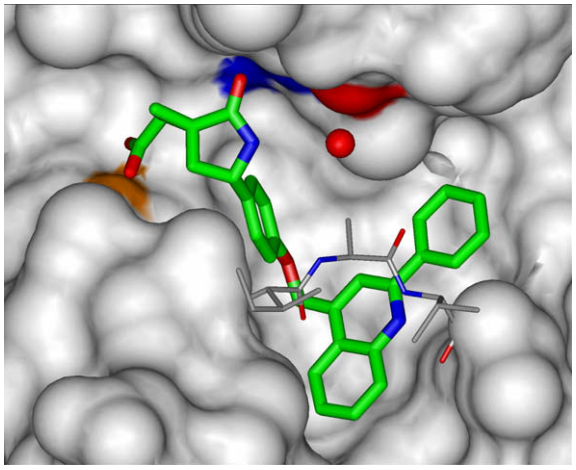

Figure 1. Crystal structure of compound **21** binding to TACE (**PDB ID**: 3EWJ). The inhibitor (green) and the flexible loop (grey) are shown as stick model. The crystal water bridging the lactam NH and the C=O of Gly346 is also shown. Note that the compound was prepared and soaked as a racemic mixture. The X-ray structure shows only the *S*-enantiomer bound.

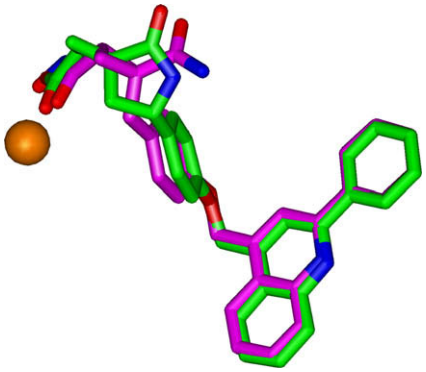

Figure 2. Overlay of the crystal structures of compounds **2** (magenta) and **21** (green). Only ligands and the active site zinc are shown for clarity.

crowding in that region. Multiple attempts to obtain a crystal structure of a hydroxamate compound from this series were unsuccessful. The crystal structure of compound **21** also indicates a small space available to accommodate the *m*-fluorine which would make favorable contacts with the side chain of Val 402. This is consistent with the increase in potency of compounds **19** versus **21**. Figure 2 shows an overlay of the crystal structure of compounds **2** and **21.** The quinoline group binds to the S1′/S3′ region in the same orientation as in the cyclopropyl series. The 2-phenyl group makes stacking interactions with the side chain of Glu398 and there is some change in location of the amide moiety relative to the lactam carbonyl. It is not obvious from the X-ray structures why compounds **22** and **25** with 4- and 3-pyridinyl would lose potency by 5- and 20-fold relative to phenyl at this position since this group is solvent exposed.

We attempted to explain the less than expected potency shift of the carboxylate- versus hydroxamate-spirocyclopropyl compounds. Because of the extra carbon spacer of the spirocyclopropyl relative to the cyclopropyl scaffolds, the P1′ group moved further toward the prime side and weakened pi–pi stacking interactions between the middle phenyl ring and His405. The phenyl group would also have steric crowding with the side chain of Ala439. On the other hand, the carboxylate zinc binding group being shorter, allows the P1′ group to move away slightly and therefore alleviate the steric conflict with Ala439.

In summary, we have reported a novel scaffold that affords potent TACE inhibition for both hydroxamate and carboxylate compounds. Carboxylate TACE inhibitors are particularly interesting because of their chemical stability and potentially favorable pharmacokinetics. Although carboxylate inhibitors binding to MMPs have been reported, there are only limited reports on binding to TACE.[17] While further work is needed to improve potency, this work opens up the possibility of designing potent and selective small molecule carboxylate TACE inhibitors.

Acknowledgments

The authors thank Dr. Corey Strickland for critical reading of the manuscript and helpful suggestions.

References and notes

1. Bemelmans, M. H.; van Tits, L. J.; Buurman, W. A. *Crit. Rev. Immunol.* **1996**, *16*, 1.
2. Aggarwal, B. B.; Natarajan, K. *Eur. Cytokine Netw.* **1996**, *7*, 93.
3. Black, R. A.; Rauch, C. T.; Kozlosky, C. J.; Peschon, J. J.; Slack, J. L.; Wolfson, M. F.; Castner, B. J.; Stocking, K. L.; Reddy, P.; Srinivasan, S.; Nelson, N.; Boiani, N.; Schooley, K. A.; Gerhart, M.; Davis, R.; Fitzner, J. N.; Johnson, R. S.; Paxton, R. J.; March, C. J.; Cerretti, D. P. *Nature* **1997**, *385*, 729.
4. Maskos, K.; Fernandez-Catalan, C.; Huber, R.; Bourenkov, G. P.; Bartunik, H.; Ellestad, G. A.; Reddy, P.; Wolfson, M. F.; Rauch, C. T.; Castner, B. J.; Davis, R.;

Clarke, H. R.; Petersen, M.; Fitzner, J. N.; Cerretti, D. P.; March, C. J.; Paxton, R. J.; Black, R. A.; Bode, W. *Proc. Natl. Acad. Sci. U.S.A.* **1998**, *95*, 3408.
5. Nemunaitis, J.; Poole, C.; Primrose, J.; Rosemurgy, A.; Malfetano, J.; Brown, P.; Berrington, A.; Cornish, A.; Lynch, K.; Rasmussen, H.; Kerr, D.; Cox, D.; Millar, A. *Clin. Cancer Res.* **1998**, *4*, 1101.
6. Wojtowicz-Praga, S.; Torri, J.; Johnson, M.; Steen, V.; Marshall, J.; Ness, E.; Dickson, R.; Sale, M.; Rasmussen, H. S.; Chiodo, T. A.; Hawkins, M. J. *J. Clin. Oncol.* **1998**, *6*, 2150.
7. List, A. F.; Kurtin, S. E.; Callander, N.; Anderson, J. E.; Foran, J. M.; Rabinowitz, I.; Glinsmann-Gibson, B. J.; Bellamy, W. T.; Bennet, J. M.; Collier, M.; Mazabel, E. *Abstract of Papers*, 44th Annual Meeting of American Society of Hematology, Philadelphia, PA, 2002; 100, Abstract 3119.
8. Zhu, Z.; Mazzola, R.; Sinning, L.; McKittrick, B.; Niu, X.; Lundell, D.; Sun, J.; Orth, P.; Guo, Z.; Madison, V.; Ingram, R.; Beyer, B. M. *J. Med. Chem.* **2008**, *51*, 725.
9. Mazzola, R.; Zhu, Z.; Sinning, L.; McKittrick, B.; Lavey, B.; Spitler, J.; Kozlowski, J.; Shih, N.-Y.; Zhou, G.; Guo, Z.; Orth, P.; Madison, V.; Niu, X.; Sun, J.; Lundell, D. *Bioorg. Med. Chem. Lett.* **2008**, *18*, 5809.
10. Duan, J. J.-W.; Chen, L.; Wasserman, Z. R.; Lu, Z.; Liu, R.-Q.; Covington, M. B.; Qian, M.; Hardman, K. D.; Magolda, R. L.; Newton, R. C.; Christ, D. D.; Wexler, R. R.; Decicco, C. P. *J. Med. Chem.* **2002**, *45*, 4954.
11. Niu, X.; Umland, S.; Ingram, R.; Beyer, B. M.; Liu, Y.-H.; Sun, J.; Lundell, D.; Orth, P. *Arch. Biochem. Biophys.* **2006**, *451*, 43.
12. Maldaner, A. O.; Pilli, R. A. *Tetrahedron* **1999**, *55*, 13321.
13. Skiles, J. W.; Gonnella, N. C.; Jeng, A. Y. *Curr. Med. Chem.* **2001**, *28*, 425.
14. Cross, J. B.; Duca, J. S.; Kaminski, J. J.; Madison, V. *J. Am. Chem. Soc.* **2002**, *124*, 11004.
15. Human whole blood is diluted 1:1 with serum free medium (RPMI, L-glutamine, Pen-Strep, HEPES) and incubated with compounds in a final volume of 360 μL for 1 h at 37 °C. Forty microliters of LPS (10 μg/ml) is then added. Supernatant is collected after 3.5 h incubation and the concentration of TNF-α is determined by ELISA (R&D Systems).
16. Ingram, R. N.; Orth, P.; Strickland, C. L.; Le, H. V.; Madison, V.; Beyer, B. M. *Protein Eng. Des. Sel.* **2006**, *19*, 155.
17. Park, K.; Levin, J. I.; Ariamala G. US2006/0160884.